

# Comparative Intra- and Inter-observer Reliability of Two Methods for Evaluating Intraoperative Ultrasonography-based Spinal Cord Hyperechogenicity Intensity in Degenerative Cervical Myelopathy

Huachuan Wu (✉ [wuhch6@mail2.sysu.edu.cn](mailto:wuhch6@mail2.sysu.edu.cn))

The Seventh Affiliated Hospital of Sun Yat-sen University

Guoliang Chen

The Seventh Affiliated Hospital of Sun Yat-sen University

Xianlong Li

The Seventh Affiliated Hospital of Sun Yat-sen University

Zhengya Zhu

The Seventh Affiliated Hospital of Sun Yat-sen University

Zuofeng Xu

The Seventh Affiliated Hospital of Sun Yat-sen University

Xizhe Liu

First Affiliated Hospital of Sun Yat-sen University

Shaoyu Liu

The Seventh Affiliated Hospital of Sun Yat-sen University

---

## Research Article

**Keywords:** degenerative cervical myelopathy, spinal cord, intraoperative ultrasound, Hyperechogenicity, intra- and interobserver reliabilities

**Posted Date:** April 19th, 2022

**DOI:** <https://doi.org/10.21203/rs.3.rs-1522935/v1>

**License:**   This work is licensed under a Creative Commons Attribution 4.0 International License.

[Read Full License](#)

---

**Version of Record:** A version of this preprint was published at BMC Musculoskeletal Disorders on September 6th, 2022. See the published version at <https://doi.org/10.1186/s12891-022-05517-0>.

# Abstract

**Objective:** To acquire a higher-reliability method, and compare the in-observer and inter-observer reliability of two methods in evaluating the hyperechoic intensity of spinal cord ultrasound in degenerative cervical myelopathy (DCM).

**Materials and Methods:** Totally 28 patients (20 males and 8 females) who had been followed up for 12 months were included. Their mean age at surgery was  $61.2 \pm 10.8$  years and the average symptom duration was  $23.36 \pm 22.11$  months. The gray values of circles 1, 2 and 3 were recorded as  $G_{\text{compression}}$ ,  $G_{\text{norml}}$  and  $G_{\text{sac}}$ , respectively. The gray value ratio (GVR) was calculated as follows:  $\text{GVR-A} = G_{\text{compression}}/G_{\text{norml}}$  (method A), and  $\text{GVR-B} = G_{\text{compression}}/G_{\text{sac}}$  (method B). The in-observer and inter-observer reliabilities of the two methods were compared. It is generally believed a reliability coefficient  $< 0.40$  and  $> 0.75$  indicate poor and good reliability respectively. The images-based GVR-B using this protocol demonstrates higher inter- and intraobserver reliabilities than GVR-A, and can be used as the basis for prognostic prediction and future studies.

**Results:** All examination acquisitions were successfully completed. GVR-A averaged 2.043 (0.318–5.56), and GVR-B averaged 0.578(0.06–1.41). GVR-B has better repeatability of gray value measurement, smaller RSD% (0.298 vs. 0.32) and larger inter-group correlation coefficient compared with GVR-A. The mean value (MD) of the GVR difference calculated by GVR-B between the two clinicians was closer to 0.

**Conclusions:** For DCM patients routinely using ultrasound for real-time cord visualization during spinal cord decompression by French-door laminoplasty, the images-based GVR-B using this protocol demonstrates better inter- and intraobserver reliabilities compared with GVR-A.

## Introduction

Degenerative cervical myelopathy (DCM) is the most common non-traumatic disorder leading to neurological dysfunction in adults [1]. For DCM, the major pathological alterations of the spinal cord include parenchymatous degeneration (ischemia and edema) and cystic necrosis caused by chronic spinal cord compression [2]. These two pathological alterations may lead to different neurological recoveries of DCM, but are always reflected as increased signal intensity (ISI) on T2W magnetic resonance imaging (MRI) [3]. The T2W signal intensity of the spinal cord is widely used to assess the impairment status and predict the neurological recovery of DCM [4], though this characteristic may influence clinical evaluation. Recently, intraoperative ultrasonography (IOUS) was preformed to evaluate and guide surgical decompression, and some IOUS-derived metrics were confirmed to be significantly correlated with the neurological function in DCM [5–6]. Like ISI on T2W MRI, the spinal cord can manifest as hyperechogenicity on IOUS, with the same segment of ISI on T2W MRI [7]. The intensity of spinal cord hyperechogenicity is considered as a potential predictive indicator of neurological recovery in DCM after decompression [8]. To avoid the deviations caused by variations among machines, operators or observers, the gray value ratio (GVR) was measured to represent the intensity of spinal cord

hyperechogenicity, by referring to the methods of measuring the signal change rate of the spinal cord on T2W MRI [9–10]. Previously, two methods of measuring GVR with different reference elements were used to analyze the correlation between GVR and postoperative neurological recovery [7–8, 11]. However, the accuracy of GVR which highly influences the accuracy of study conclusions may be subjected to many factors, especially the selections of region of interest (ROI) that differ among observers and among assessing timings of the same observer. Herein, we compared intra- and inter-observer reliabilities of two methods in evaluating the intraoperative ultrasonography based spinal cord hyperechogenicity intensity in DCM, aiming to find out a more reliable method. The results originating from this method are expected to be the basis of further studies.

## Materials And Methods

### Study population

This study was approved by the Institutional Review Board of the studied hospital. Signed informed consents were obtained from all participants after explanation of the conductors.

A total of 33 consecutive patients with multilevel DCM ( $\geq 3$ ) were prospectively enrolled between October 2018 and September 2019. Patients with a history of other spinal disorders, neurological injury, infection, tumor, or rheumatoid arthritis were excluded. Finally, 28 patients (20 males and 8 females) who had been followed up for 12 months were included. Their mean age at surgery was  $60.8 \pm 10.3$  years and the average symptom duration was  $40.7 \pm 34.1$  months (Table 1).

**Table 1**

Demographic data of patients

indicator	result
number of case	28
gender (male/female)	20/8
age at surgery (years)	$61.2 \pm 10.8$
symptom duration (months)	$23.36 \pm 22.11$

### Image acquisition

IOUS images were collected by the same surgeon in performing French-door laminoplasty according to Kurokawa's method with some modifications [12]. After the detachment of bilateral paravertebral muscles, the centers of spinous processes were cut using a self-create and patented fretsaw. Bilateral gutters were created as hinges at the border of the laminae and facets. After the halves of the laminae

were elevated and fixed to bilateral skin provisionally, normal saline was infused to form an acoustic window, then a linear array transducer of IOUS was used to observe the spinal cord and record the images. If residual compression was observed, further decompression under IOUS guidance was done. After observation, the appropriately- sized hydroxyapatite spacers were tied in place to bridge the bilateral edges of the laminae and were fixed with wires. Finally, a drainage tube was placed and the wound was closed in layers.

## IOUS measurements

The measurement protocol was formulated according to the experimental purposes above. The gray value of each ROI was measured by ImageJ (National Institutes of Health, Bethesda, MD, USA). All midsagittal images of the spinal cord (midsagittal slice was determined by visualizing the central echo complex of spinal cord) used to measure the GVR of hyperechogenicity were selected independently by the same two experienced surgeons who took part in the surgery. The GVRs of the two methods were measured independently by the same two researchers (a spine surgeon and a sonographer) and repeated three times (the interval between two measurements was not less than 7 days), following the same routine and using the same computer and software. For patients with macroscopic hyperechogenicity on IOUS, circle 1 was drawn with the maximum brightness point within the spinal cord as the center, circle 2 with the same area was plotted on the spinal cord with uniform echogenicity, without compression and at least 1 cm away from the circle 1, and circle 3 was drawn on the dorsal dural sac at the same segment as circle 1. For patients without different echogenicity within the spinal cord, circle 1 was drawn within the spinal cord at the most compressed level, and circles 2 and 3 were plotted according to the methods described previously. Importantly, the central canal of the spinal cord must be avoided in the drawing of circles 1 and 2. The gray values of circles 1, 2 and 3 were recorded as  $G_{\text{compression}}$ ,  $G_{\text{norml}}$  and  $G_{\text{sac}}$ , respectively (Figure 1A & 1B). GVR was calculated as follows:  $\text{GVR-A} = G_{\text{compression}}/G_{\text{norml}}$  (method A), and  $\text{GVR-B} = G_{\text{compression}}/G_{\text{sac}}$  (method B).

## Statistical analysis

Statistical analysis was carried out with IBM SPSS statistical software version 22.0 (IBM Corp., Armonk, NY, USA). Data were expressed as mean  $\pm$  standard deviation (SD). The intra- and interobserver reliabilities of the gray value parameter measurements were quantified using the intraclass correlation coefficient (ICC), with a confidence interval of 95%. ICC, the full name is intraclass correlation coefficient, is one of the important reliability coefficient indicators for measuring and evaluating inter-observer reliability and test-retest reliability. ICC of 0.00 - 0.20, 0.21 - 0.40, 0.41 - 0.60, 0.61 - 0.80, and 0.81 - 1.00 is considered slight, fair, moderate, substantial, and almost perfect agreement respectively [13-14]. It is generally believed that a reliability coefficient  $< 0.40$  and  $> 0.75$  indicates poor and good reliability respectively. For quantitative data, higher ICC is often required. The means of GVR were compared by T-TEST PAIRS. P values less than 0.05 were considered significant. To further acquire and illustrate a

calculating method of GVR with higher reliability, we also adopted Bland-Altman analysis to account for the said results.

## Results

According to the formula to calculate the GVR, The GVR-A averaged 2.043 (0.318–5.56), GVR-B averaged 0.578 (0.06–1.41) after surgery.

## Ultrasonic signal Parameters

Based on the calculating methods of GVR,  $G_{norml}$  and  $G_{sac}$  were recorded three times at least one week apart. For the gray value, the intra-observer reliability was classified at different corresponding observation areas (Table 2).

Table 2  
Comparison of results of gray value measured by observer A and observer B

method	n	Observer A ICC (95%CI)	Observer B ICC (95%CI)
$G_{compression}$	28	0.85 (0.741–0.921)	0.979 (0.962–0.99)
$G_{norml}$	28	0.826 (0.706–0.908)	0.922 (0.86–0.96)
$G_{sac}$	28	0.794 (0.652–0.891)	0.874 (0.781–0.934)
<i>(CI: confidence interval; ICC: intraclass confidence correlation)</i>			

At the maximum brightness point within the spinal cord, the intra-observer reliability of  $G_{compression}$  was classified as “almost perfect agreement” (Observer A ICC (95% CI): ICC0.85, ICC = 0.741–0.921; Observer B ICC (95%CI): ICC 0.979, ICC = 0.962–0.99, both  $P < 0.001$ ) (Table 2).

At the spinal cord with uniform echogenicity, the intra-observer reliability of  $G_{norml}$  was also classified as “almost perfect agreement” (Observer A ICC (95%CI):ICC0.826, ICC = 0.706–0.908; Observer B ICC (95% CI): ICC0.922, ICC = 0.86-0.96, both  $P < 0.001$ ) (Table 2).

On the dorsal dural sac at the same segment with circle 1, and the maximum brightness point within the spinal cord, the intra-observer reliability of  $G_{sac}$  from Observer A resulted in “substantial agreement” (ICC (95%CI): ICC0.794, ICC =0.652–0.891,  $P < 0.001$ ), and the reliability coefficient still exceeds 0.75, indicating good reliability. Moreover, the intra-observer reliability of Observer B resulted in “almost perfect agreement” (ICC (95%CI): ICC 0.874, ICC = 0.781–0.934,  $P < 0.001$ ) (Table 2).

## Intraobserver Reliability

For GVR-A, the intraobserver reliability was classified as “moderate agreement” (Observer A ICC (95% CI): ICC 0.596, ICC = 0.391–0.767; Observer B ICC(95%CI): ICC 0.595, ICC = 0.387–0.767, both P < 0.001) (Table 3).

Table 3  
Intraobserver reliability of GVR-A and GVR-B

method	n	Observer A ICC (95%CI)	Observer B ICC (95%CI)
GVR-A	28	0.596 (0.391–0.767)	0.595 (0.387–0.767)
GVR-B	28	0.752 (0.594–0.866)	0.89 (0.807–0.943)
<i>(GVR-A = <math>G_{compression}/G_{norm}</math>, GVR-B = <math>G_{compression}/G_{sac}</math>; CI: confidence interval; ICC: intraclass confidence correlation).</i>			

For GVR-B, the intraobserver reliability was good (Observer A ICC (95% CI): ICC 0.752, ICC = 0.594–0.866; Observer B ICC(95%CI): ICC 0.89, ICC = 0.807–0.943, both P < 0.001) (Table 3).

## Interobserver Reliability

For GVR-A, interobserver reliability was classified as “slight agreement” (ICC (95%CI): ICC 0.198, ICC = -0.183–0.527, P < 0.001) (Table 4).

Table 4  
Interobserver Reliability of GVR-A and GVR-B

method	n	Interobserver Reliability ICC (95% CI)
GVR-A	28	0.198 (-0.183-0.527)
GVR-B	28	0.86 (0.72–0.933)
<i>(GVR-A = <math>G_{compression}/G_{norm}</math>, GVR-B = <math>G_{compression}/G_{sac}</math>; CI: confidence interval; ICC: intraclass confidence correlation)</i>		

For GVR-B, interobserver reliability was classified as “substantial to almost perfect agreement” (ICC (95%CI): ICC0.86, ICC = 0.72–0.933, P < 0.001) (Table 4).

## Comparison of two methods in calculating GVR

According to the comparison of the two methods in calculating GVR (Table 5), the image-based GVR-B using this protocol has better repeatability, smaller RSD%, and larger ICC compared with GVR-A. The practical reliability significantly differs between the two methods (P < 0.05). The distribution results of GVR-A and GVR-B are shown in Fig. 2A and 2B.

Table 5  
Comparison of two methods of calculating GVR ( $\bar{x} \pm s$ )

method	n	Observer A	Observer B	RSD%
<i>GVR-A</i>	28	1.837±0.671	2.25±0.577	0.32
<i>GVR-B</i>	28	0.555±0.157	0.602±0.186	0.298
t		10.298	-2.77	
p		0	0.01	
<i>(GVR-A = <math>G_{compression}/G_{norm}</math>, GVR-B = <math>G_{compression}/G_{sac}</math>)</i>				

Furthermore, the two methods of measuring the GVR difference of the spinal cord were compared by Bland-Altman analysis (Table 6, Fig. 2A&2B and 2C). The mean value (MD) of the GVR difference calculated by GVR-B between the two clinicians was closer to 0 and smaller than that from GVR-A. It can be seen that compared with the GVR-A method, the method GVR-B has a higher consistency in measurement.

Table 6  
Bland Altman analysis results of the GVR under two measurement methods

Items	GVR-A	GVR-B
MD	-0.413(-0.72 - -0.106)	-0.048(-0.083 - -0.0124)
lower limit of 95% LoA	1.14(0.608-1.671)	-0.227(-0.288 - -0.165)
upper limit of 95% LoA	-1.966(-2.497 - -1.434)	0.131(0.07-0.192)
t	-2.759	-2.77
P	0.01	0.01
<i>(GVR-A:GVR-A = <math>G_{compression}/G_{norm}</math>, GVR-A:GVR-B = <math>G_{compression}/G_{sac}</math>; 95% LoA:95% limits of agreement).</i>		

## Discussion

The gray values of different spinal cord elements including the maximal compressive level, compression-free level and the dural sac were measured, and the GVRs of maximal compressive level/compression free level and maximal compressive level/dural sac were calculated. The results of intra- and inter-observer reliability prove that the GVR of maximal compressive level/dural sac is more consistent for both inter- and intra-observer reliability.

In DCM, owing to the chronic compression, many pathological changes occur in the spinal cord, including ischemia, edema, neuron apoptosis, spinal cord atrophy and cystic necrosis [15]. Consistently, these pathological changes are always reflected as ISI on T2W MRI. This characteristic of MRI may cause the deviation when the signal intensity of T2W MRI ISI is used to evaluate the status and predict the neurological recovery of DCM. The parenchymatous degeneration and cystic necrosis indicate different severities of spinal cord impairment [16-17]. The cystic necrosis of the spinal cord can also be reflected as T1W hypointensity, but the positive rate of T1W hypointensity is not high in DCM. This characteristic limits the application of T1W MRI in DCM [18].

The echogenicity of ultrasonography is based on the different densities of tissues (Walker 2004). For DCM, the chronic compression derived pathological changes may cause different densities of the spinal cord [19]. Then the different densities of the spinal cord are reflected as different levels of echogenicity on IOUS. Previously, we quantified the spinal cord hyperechogenicity as gray value, and revealed the negative correlation between hyperechogenicity intensity and postoperative neurological recovery [7-8]. Besides, ultrasound has a significant image difference between liquid and parenchymal tissues, and thus can easily identify the pathology of cystic and parenchymatous changes. All those features of

ultrasonography are unfulfilled on the clinical application of MRI or CT, and determine the application value and irreplaceability of IOUS.

According to the ultrasonography principles, differences in the density of adjacent tissues result in different echoes and are reflected as different gray values on ultrasound images [20]. The spinal cord hyperechogenicity in DCM patients results from the chronic compression subjected to the static and dynamic mechanical forces acting on the spinal cord [21-22]. The chronic compression leads to fibrin deposition, and even fibrosis in the compression region, accompanied with the loss of nerve cells, proliferative fibroblasts and capillary endothelial cells [23-24]. Eventually, the uneven density of the spinal cord will occur and appears as hyperechogenicity on IOUS [25-26]. As shown in the typical case, spinal ultrasound can still detect signs that are not observed by MRI. When MRI presents only high signal changes, ultrasound can still return additional signs, such as syringomyelia signs. The intensity of spinal cord hyperechogenicity is considered as a potential predictor of neurological recovery in DCM after decompression. Therefore, the reliabilities of two methods to evaluate the hyperechoic intensity of DCM spinal ultrasound in the same observer and between observers were compared to find out a more reliable evaluation method.

The method used to calculate GVR by comparing the gray values of spinal cord hyperechogenicity and dural sac (GVR-B) is highly consistent for both inter- and intra-observer reliabilities, which are obviously higher than those of GVR-A. We attributed this improvement to the selection of ROIs, which, for intraoperative ultrasonic signal measurement, may be an important influence factor on GVR.  $G_{\text{compression}}$  (gray value of circle 1) has a one-to-one correspondence with  $G_{\text{sac}}$  (gray value of circle 3), but  $G_{\text{norml}}$  (gray value of circle 2) does not have such correspondence with  $G_{\text{sac}}$ . The principle of ROI selection and the GVR-based calculation method reflect that  $G_{\text{norml}}$  is more random and highly variable, which also result in lower reliability of GVR-A. Conversely, when GVR-B was used to calculate the same  $G_{\text{compression}}$ , more significant intra- and inter-observer reliability was obtained, indicating its consistency is better with the dura mater as a reference. Based on this finding, we suggest to use method B to evaluate the intensity of spinal cord hyperechogenicity in DCM.

There are several main limitations. First, as an exploratory prospective study, the sample size was relatively small. Second, no patient-based outcomes were evaluated. Moreover, the lack of multicenter study can lower the reliability of our statistical analysis.

## Conclusions

The parameters of IOUS echogenicity measurement show high reliability both within and between observers. Our collective data support that the images-based GVR-B using this protocol has higher inter- and intra-observer reliabilities compared with GVR-A, and may be used as the basis for future studies.

## Declarations

## **Ethics approval and consent to participate**

This study was reviewed and approved by the Institutional Review Board and Ethics Committee of the Seventh Affiliated Hospital of Sun Yat-sen University in Shenzhen, China. Signed informed consents were obtained from all participants after explanation of the conductors. All methods were carried out in accordance with relevant guidelines and regulations.

## **Consent for publication**

Not applicable.

## **Availability of data and material**

The datasets used and/or analyzed during the current study are available from the corresponding author on necessary and reasonable request.

## **Conflicts of interest statement**

The funding bodies were not involved in the decision-making of this study, and all authors declare no conflicts of interest to disclose.

## **Funding information**

Funding for this study was received from the Sanming Project of Medicine in Shenzhen (No. SZSM201911002), Sun Yat-sen University Clinical Research 5010 Program (No. 2019009).

## **Author contributions:**

Guarantor of integrity of entire study, study concepts/study design, experimental studies, and literature research, all authors;

Conceptualization: Huachuan Wu, Guoliang Chen, Xizhe Liu, Shaoyu Liu. Data curation: Huachuan Wu, Guoliang Chen, Xianlong Li, Zhengya Zhu. Formal analysis: Huachuan Wu, Zhengya Zhu. Funding acquisition: Shaoyu Liu. Investigation: Huachuan Wu, Guoliang Chen, Xianlong Li. Methodology: Huachuan Wu, Guoliang Chen. Project administration: Xizhe Liu, Zuofeng Xu, Shaoyu Liu. Resources: Xizhe Liu, Zuofeng Xu, Shaoyu Liu. Software: Huachuan Wu, Guoliang Chen, Xianlong Li. Supervision: Xizhe Liu, Zuofeng Xu, Shaoyu Liu. Validation: Huachuan Wu, Guoliang Chen, Xizhe Liu. Visualization: Guoliang Chen, Xizhe Liu. Writing—original draft: Huachuan Wu, Guoliang Chen. Writing—review & editing: Xizhe Liu, Zuofeng Xu, Shaoyu Liu.

## **Acknowledgments:**

This work was supported by the Sanming Project of Medicine in Shenzhen (SZSM201911002). We thank Zuofeng Xu, MD for their technical support and helpful discussions in intraoperative ultrasound imaging.

## References

1. Badhiwala JH, Ahuja CS, Akbar MA, Witiw CD, Nassiri F, Furlan JC, Curt A, Wilson JR, Fehlings MG. Degenerative cervical myelopathy - update and future directions. *Nat Rev Neurol* 2020; 16:108-24.
2. White AA, Panjabi MM. Biomechanical considerations in the surgical management of cervical spondylotic myelopathy. *Spine* 1988; 13:856-60.
3. Machino M, Ando K, Kobayashi K, Ito K, Tsushima M, Morozumi M, Tanaka S, Ota K, Ito K, Kato F, Ishiguro N, Imagama S. Alterations in Intramedullary T2-weighted Increased Signal Intensity following Laminoplasty in Cervical Spondylotic Myelopathy Patients: Comparison Between Pre- and Postoperative Magnetic Resonance Images. *Spine (Phila Pa 1976)* 2018; 43:1595-601.
4. Nouri A, Tetreault L, Dalzell K, Zamorano JJ, Fehlings MG. The Relationship Between Preoperative Clinical Presentation and Quantitative Magnetic Resonance Imaging Features in Patients With Degenerative Cervical Myelopathy. *Neurosurgery* 2017; 80:121-28.
5. Chen G, Wei F, Shi L, Li J, Wang X, Wang M, Wu H, Xu Z, Liu X, Liu S. Inadequate spinal cord expansion in intraoperative ultrasound after decompression may predict neurological recovery of degenerative cervical myelopathy. *European Radiology* 2021.
6. Schär RT, Wilson JR, Ginsberg HJ. Intraoperative Ultrasound-Guided Posterior Cervical Laminectomy for Degenerative Cervical Myelopathy. *World Neurosurgery* 2019; 121:62-70.
7. Chen G, Li J, Wei F, Ji Q, Sui W, Chen B, Zou X, Xu Z, Liu X, Liu S. Short-term predictive potential of quantitative assessment of spinal cord impairment in patients undergoing French-door Laminoplasty for degenerative cervical myelopathy: preliminary results of an exploratory study exploiting intraoperative ultrasound data. *BMC musculoskeletal disorders* 2020; 21:336.
8. Chen G, Wei F, Li J, Shi L, Zhang W, Wang X, Xu Z, Liu X, Zou X, Liu S. Intensity of Intraoperative Spinal Cord Hyperechogenicity as a Novel Potential Predictive Indicator of Neurological Recovery for Degenerative Cervical Myelopathy. *Korean journal of radiology* 2021; 22:1163-71.
9. Karpova A, Arun R, Cadotte DW, Davis AM, Kulkarni AV, O'Higgins M, Fehlings MG. Assessment of spinal cord compression by magnetic resonance imaging—can it predict surgical outcomes in degenerative compressive myelopathy? A systematic review. *Spine (Phila Pa 1976)* 2013; 38:1409-21.
10. Wang LF, Zhang YZ, Shen Y, Su YL, Xu JX, Ding WY, Zhang YH. Using the T2-weighted magnetic resonance imaging signal intensity ratio and clinical manifestations to assess the prognosis of patients with cervical ossification of the posterior longitudinal ligament. *J Neurosurg Spine* 2010; 13:319-23.
11. Chen G, Wu H, Chen N, Wang M, Shi L, Li J, Wei F, Xu Z, Liu X, Liu S. Potential of Intraoperative Ultrasonographic Assessment of Spinal Cord Central Echo Complex in Predicting Postoperative Neurological Recovery of Degenerative Cervical Myelopathy. *European journal of neurology* 2021.
12. Kurokawa T TN, Tanaka H, Kobayashi M, Machida H, Izuka T, Hoshino Y, Hatsuyama Y. Enlargement of the spinal canal by the sagittal splitting of the spinous processes. *Bessatsu Seikeigeka* 1982;

2:234-40.

13. Koo TK, Li MY. A Guideline of Selecting and Reporting Intraclass Correlation Coefficients for Reliability Research. *J Chiropr Med* 2016; 15:155-63.
14. Martin AR, Jentzsch T, Wilson JRF, Moghaddamjou A, Jiang F, Rienmuller A, Badhiwala JH, Akbar MA, Nater A, Oitment C, Ganau M, Massicotte EM, Fehlings MG. Inter-Rater Reliability of the Modified Japanese Orthopaedic Association Score in Degenerative Cervical Myelopathy: A Cross-Sectional Study. *Spine* 2021.
15. David G, Mohammadi S, Martin AR, Cohen-Adad J, Weiskopf N, Thompson A, Freund P. Traumatic and nontraumatic spinal cord injury: pathological insights from neuroimaging. *Nat Rev Neurol* 2019; 15:718-31.
16. Ito K, Imagama S, Ito K, Ito Z, Ando K, Kobayashi K, Hida T, Tsushima M, Ishikawa Y, Matsumoto A, Machino M, Nishida Y, Ishiguro N, Kato F. MRI Signal Intensity Classification in Cervical Ossification of the Posterior Longitudinal Ligament: Predictor of Surgical Outcomes. *Spine (Phila Pa 1976)* 2017; 42:E98-E103.
17. Mizuno J, Nakagawa H, Inoue T, Hashizume Y. Clinicopathological study of "snake-eye appearance" in compressive myelopathy of the cervical spinal cord. *J Neurosurg* 2003; 99:162-68.
18. De la Garza Ramos R, Nouri A, Nakhla J, Echt M, Gelfand Y, Patel SK, Nasser R, Cheng JS, Yassari R, Fehlings MG. Predictors of Return to Normal Neurological Function After Surgery for Moderate and Severe Degenerative Cervical Myelopathy: An Analysis of A Global AOSpine Cohort of Patients. *Neurosurgery* 2019; 85:E917-E23.
19. Nouri A, Tetreault L, Singh A, Karadimas SK, Fehlings MG. Degenerative Cervical Myelopathy: Epidemiology, Genetics, and Pathogenesis. *Spine (Phila Pa 1976)* 2015; 40:E675-93.
20. Walker FO. Neuromuscular ultrasound. *Neurologic clinics* 2004; 22.
21. Baron EM, Young WF. Cervical spondylotic myelopathy: a brief review of its pathophysiology, clinical course, and diagnosis. *Neurosurgery* 2007; 60:S35-41.
22. Karadimas SK, Gatzounis G, Fehlings MG. Pathobiology of cervical spondylotic myelopathy. *Eur Spine J* 2015; 24 Suppl 2:132-8.
23. Bohlman HH, Emery SE. The pathophysiology of cervical spondylosis and myelopathy. *Spine* 1988; 13:843-46.
24. Vidal PM, Karadimas SK, Ulndreaj A, Laliberte AM, Tetreault L, Forner S, Wang J, Foltz WD, Fehlings MG. Delayed decompression exacerbates ischemia-reperfusion injury in cervical compressive myelopathy. *JCI Insight* 2017; 2.
25. Gupta R, Rummler L, Steward O. Understanding the biology of compressive neuropathies. *Clin Orthop Relat Res* 2005:251-60.
26. Rempel D, Dahlin L, Lundborg G. Pathophysiology of nerve compression syndromes: response of peripheral nerves to loading. *The Journal of bone and joint surgery. American volume* 1999; 81:1600-10.

# Figures

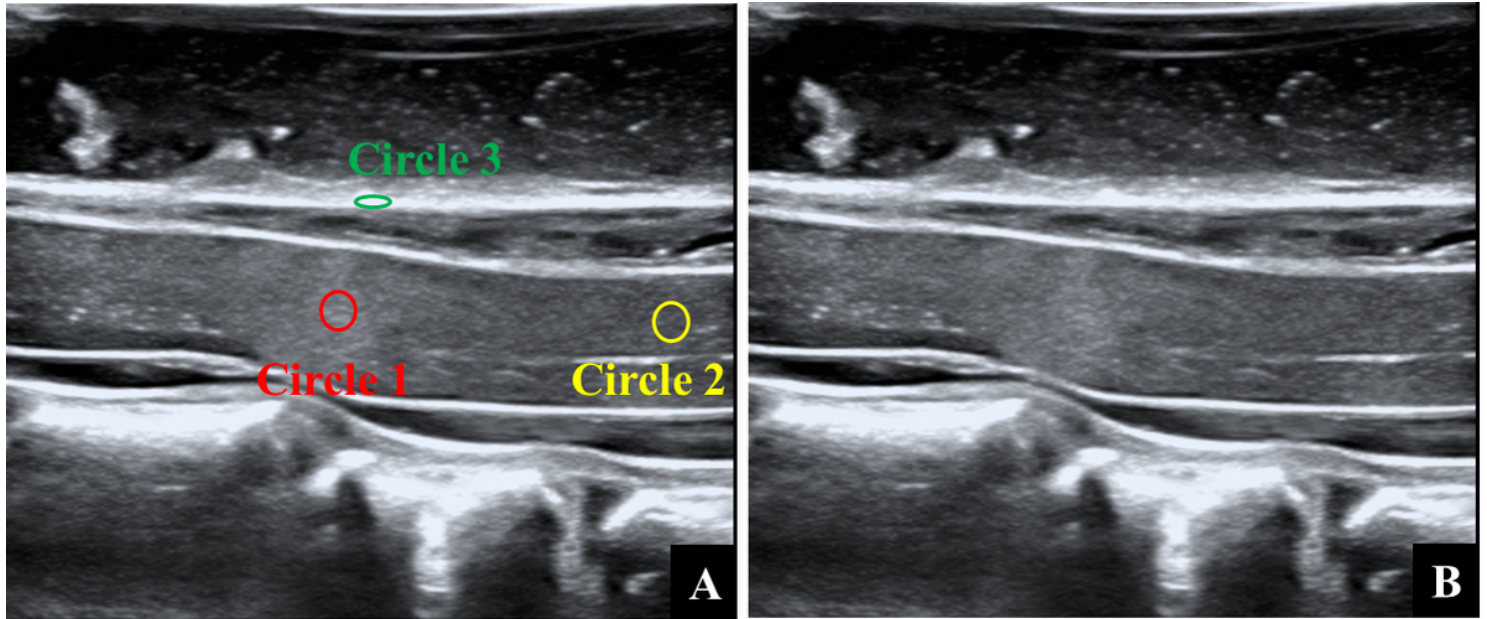


**Figure 1**

Measurements of echogenicity intensity: **(1a)**. Circle 1 (red) indicates hyperechogenicity intensity at the site of maximum compression level. Circle 2 (yellow) indicates echogenicity intensity at the site of compression-free level. Circle 3 (green) indicates echogenicity intensity of dural sac. **(1b)**. Original image of (1a) without marks.

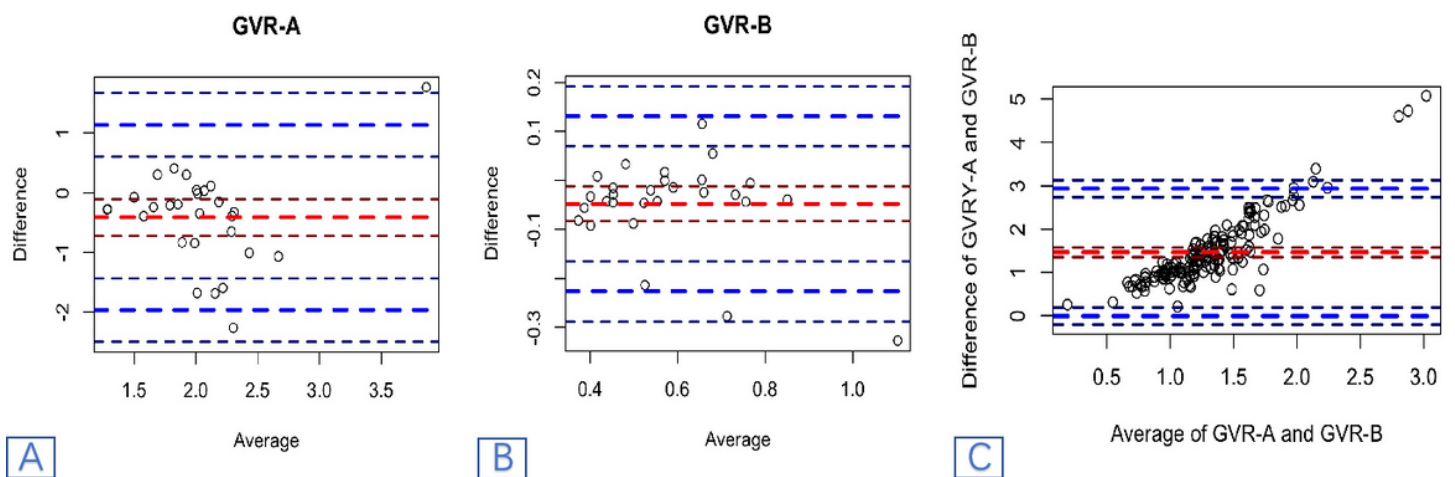


**Figure 2**

Comparison of two methods in calculating *GVR*. **(2a)**. Distribution results of *GVR-A*: x-axis and y-axis are the mean value and difference value of *GVR-A*, respectively; **(2b)**. Distribution results of *GVR-B*: x-axis and y-axis are the mean value and difference value of *GVR-B*, respectively; **(2c)**. Bland Altman analysis of

results of GVR under two measurement methods: x-axis and y-axis are the mean value and difference value of  $GVR-A + GVR-B$ , respectively.